

## **Unlocking Enhanced Electrochemical Performance through Oxygen-Nitrogen Dual Functionalization of Iron-Nickel-Sulfide for Efficient Energy Storage System**

Lan Nguyen<sup>†,a</sup>, Roshan Mangal Bhattarai<sup>†,a</sup>, Sosiawati Teke<sup>a</sup>, Kisan Chhetri<sup>b</sup>, Debendra Acharya<sup>b</sup>,  
Ragu Sasikumar<sup>c,d,e</sup>, and Young Sun Mok<sup>\*a</sup>

<sup>a</sup> Department of Chemical Engineering, Jeju National University, Jeju, Republic of Korea.

<sup>b</sup> Department of Nano Convergence Engineering, Jeonbuk National University, Jeonju, Republic of Korea.

<sup>c</sup> School of Mechatronics Engineering, Korea University of Technology and Education, Cheonan, Republic of Korea

<sup>d</sup> Advanced Technology Research Centre, Korea University of Technology and Education, Cheonan, Chungnam, Republic of Korea

<sup>e</sup> Centre of Molecular Medicine and Diagnostics, Saveetha Dental College and Hospitals, Saveetha Institute of Medical and Technical Sciences, Saveetha University, Chennai, India

<sup>†</sup>Lan Nguyen and Roshan Mangal Bhattarai contributed equally to this study.

E-mail: [smokie@jejunu.ac.kr](mailto:smokie@jejunu.ac.kr); Fax: +82-64-755-3670; Tel: +82-64-754-3682

## **1. Experimental**

### **1.1 Physical characterizations**

The structural morphologies of the samples were observed with transmission electron microscopy (TEM, Talos F200X G2, Jeju National University and JEOL JEM-2100F, Daegu Center of the Korea Basic Science Institute) operating at 200 kV and field emission scanning electron microscopy (FE-SEM) (TESCAN, MIRA3, Jeju National University, South Korea). The chemical compositions were evaluated by energy-dispersive spectroscopy (EDS) measurements and element mapping (TESCAN, MIRA) measurements at 15 kV. High-resolution (HR) brightfield imaging and combined high-angle annular dark-field (HAADF) scanning were also performed with Thermo Scientific Talos F200X G2 (Jeju National University, South Korea). X-ray diffraction (XRD) analysis was performed by using PANanalytical's Empyrean XRD with Cu K $\alpha$  ( $\lambda=0.15405$  nm) radiation in the scan range ( $2\theta$ ) of  $10^\circ$  to  $90^\circ$ . X-ray photoelectron spectroscopy (XPS) was conducted using a Theta Probe K-ALPHA+XPS system (Thermo Fisher Scientific.) with monochromatic Al K $\alpha$  at a wavelength of 1486.6 eV at 12 kV, KBSI (Korea Basic Science Institute, Busan Center).

### **1.2 Electrochemical measurements**

Electrochemical measurements such as cyclic voltammetry (CV), galvanostatic charge-discharge (GCD), and electrochemical impedance spectroscopy (EIS), were carried out using an Auto-Lab PGSTAT204N, Metrohm electrochemical workstation. These measurements were conducted using a three-electrode system, where different working electrodes were used as mentioned in their corresponding sections for different analyses. Platinum wire (2 mm  $\times$  10 mm) and Ag/AgCl were used as counter and reference electrodes respectively. 3M KOH was used as an electrolyte

throughout the electrochemical characterization. The operating parameters for different electrochemical analyses such as potential window, scan rates, current densities, etc. are mentioned in the corresponding sections.

### 1.3 Calculations

The specific capacity of various electrodes was determined utilizing Equation (S1), employing the integral area of the discharge curve derived from GCD data:

$$C_a = \frac{2i \int V dt}{S \Delta V} \quad (S1)$$

where  $C_a$  represents the areal capacity ( $\mu\text{Ah cm}^{-2}$ ),  $i$  is the applied current(A),  $\int V dt$  is the integral area of the discharge curve (V s),  $S$  denotes the area of the working electrode ( $\text{cm}^2$ ), and  $\Delta V$  signifies the voltage difference in the discharge plot (V).

The specific capacity, energy density, and power density of the ASCD were derived from the discharge time extracted from the GCD plot, utilizing the following formulas [39]:

$$C_{\text{ASCD}} = \frac{2I \int V dt}{A \Delta V} \quad (S2)$$

$$E = \frac{I \int V dt}{A} \quad (S3)$$

$$P = \frac{E}{t} \quad (S4)$$

where  $C_{ASCD}$  represents the areal capacity ( $\mu\text{Ah cm}^{-2}$ ),  $E$  denotes the energy density ( $\mu\text{Wh cm}^{-2}$ ),  $P$  signifies the power density ( $\mu\text{W cm}^{-2}$ ),  $I$  is the discharge current (A),  $\int Vdt$  is the area under the discharge curve (V s),  $A$  is the total area of the substrate covered by the active material ( $\text{cm}^2$ ),  $\Delta V$  represents the voltage difference in the discharge (V), and  $t$  is the discharge time (s) of the ASCD.

Likewise, the Electrochemical Surface Area (ECSA) of different electrodes was determined by measuring the double-layer capacitance ( $C_{dl}$ ) from the non-faradaic regions of CV curves at scan rates ranging from  $10 \text{ mV s}^{-1}$  to  $100 \text{ mV s}^{-1}$ , as demonstrated in Figure S6. As governed by Equation S5, the ECSA is directly proportional to  $C_{dl}$ . This relationship allows the electrocatalytic activity of the fabricated electrodes to be interpreted based on  $C_{dl}$  values, avoiding any misinterpretation due to uncertainty in the specific capacitance ( $C_s$ ) of the material:

$$ECSA = \frac{C_{dl}}{C_s} \quad (S5)$$

#### 1.4 Materials

Iron (III) nitrate nonahydrate ( $\text{Fe}(\text{NO}_3)_3 \cdot 9\text{H}_2\text{O}$ ,  $\geq 98\%$ ), nickel nitrate hexahydrate ( $\text{Ni}(\text{NO}_3)_2 \cdot 6\text{H}_2\text{O}$ ), Ammonium Fluoride ( $\text{NH}_4\text{F}$ ,  $\geq 98\%$ ), Hydro chloric acid (HCl), potassium hydroxide (KOH,  $\geq 95\%$ ), were purchased from Dae-Jung Chemicals & Metals Co. Ltd., South Korea. Urea ( $\text{NH}_2\text{CONH}_2$ , 99%), and ethanol ( $\text{C}_2\text{H}_5\text{OH}$ , 99.5%) were obtained from Samchun, South Korea. All the chemical compounds were analytical grade and were used without further purification. De-ionized water was used to make all aqueous solutions.

#### 1.5 Electrode preparation

### **1.5.1 Substrate preparation (NF)**

Before proceeding, the NF was treated with HCL to remove any oxide layers as well as other impurities deposited on the foam. In a typical process, a  $1 \times 1 \text{ cm}^2$  NF piece was immersed in a 3.0 M HCl solution and sonicated for 15 minutes. The obtained NF was washed several times with DI water and ethanol. The cleaned NF was then dried in a vacuum oven at  $70 \text{ }^\circ\text{C}$  for 12 hrs.

### **1.5.2 Synthesis of FNM on NF**

FNM was synthesized by growing FeNi LDH over NF substrate and subsequent annealing at high temperatures. Firstly, 1 mmol  $\text{Fe}(\text{NO}_3)_3 \cdot 9\text{H}_2\text{O}$  and 1 mmol  $\text{Ni}(\text{NO}_3)_2 \cdot 6\text{H}_2\text{O}$  were dissolved with urea (5 mmol), and  $\text{NH}_4\text{F}$  (1.5 mmol) in 40 mL DI water by using a magnetic stirrer for 30 minutes. After stirring, the solutions were transferred into the 150 mL Teflon tube containing NF and hydrothermally treated for 12 h at  $150 \text{ }^\circ\text{C}$ . After cooling to room temperature, the FeNi-LDH grown NF (named FNLDH) was washed several times with DI water, and ethanol and dried at  $70 \text{ }^\circ\text{C}$  overnight. Finally, the FNLDH was calcined at  $400 \text{ }^\circ\text{C}$  for 1 hour under a 100 sccm ammonia-nitrogen mix gas to get Fe/Ni nanosheets alloy, and the sample was named FNM. The oxygen functionalized sample (FNMO) was obtained by calcinating the FNM in the air at  $400 \text{ }^\circ\text{C}$  for 1 hour.

### **1.5.3 Synthesis of FNMS and FNMOS**

The FNM and FNMO samples were then sulfurized under hydrothermal conditions with thioacetamide (0.15g) in DI water (40 mL) at  $120 \text{ }^\circ\text{C}$  for 5 hours. Later the sulfurized samples were taken out of the hydrothermal reaction vessel, washed with DI water and ethanol, and dried at  $70 \text{ }^\circ\text{C}$  overnight to finally get FNMS and FNMOS respectively.

#### **1.5.4 Preparation of the negative electrode (CFAC)**

To use the CFAC as the negative electrode in a supercapacitor device, the CFAC was mixed with PVDF and super P at a ratio of 80:10:10 with NMP and brush coated onto the NF substrate of  $1 \times 1 \text{ cm}^2$ . The electrode was dried in a vacuum oven at  $100 \text{ }^\circ\text{C}$  for 10 h.

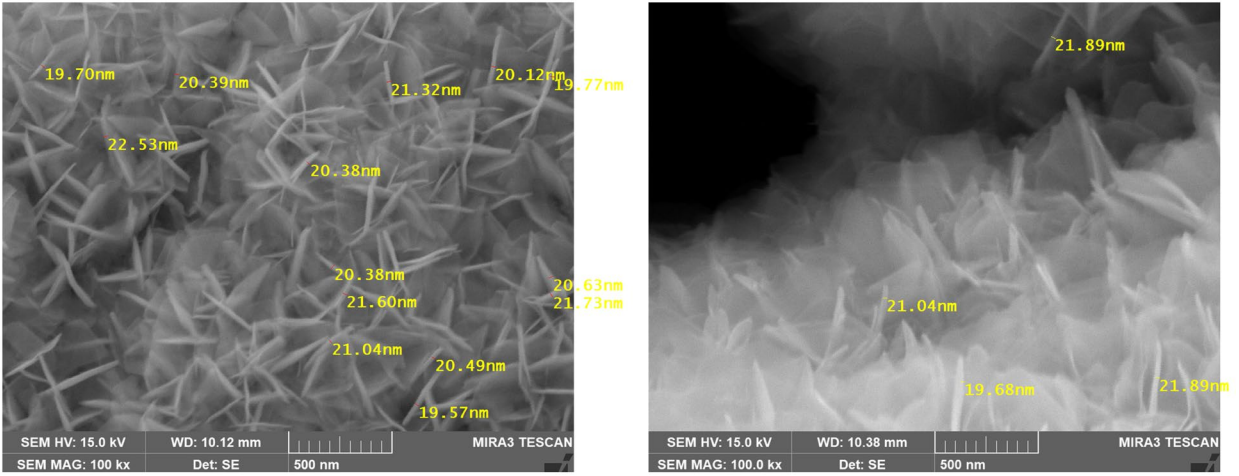


**Figure S1.** Thickness measurement of the FNM nanosheets.

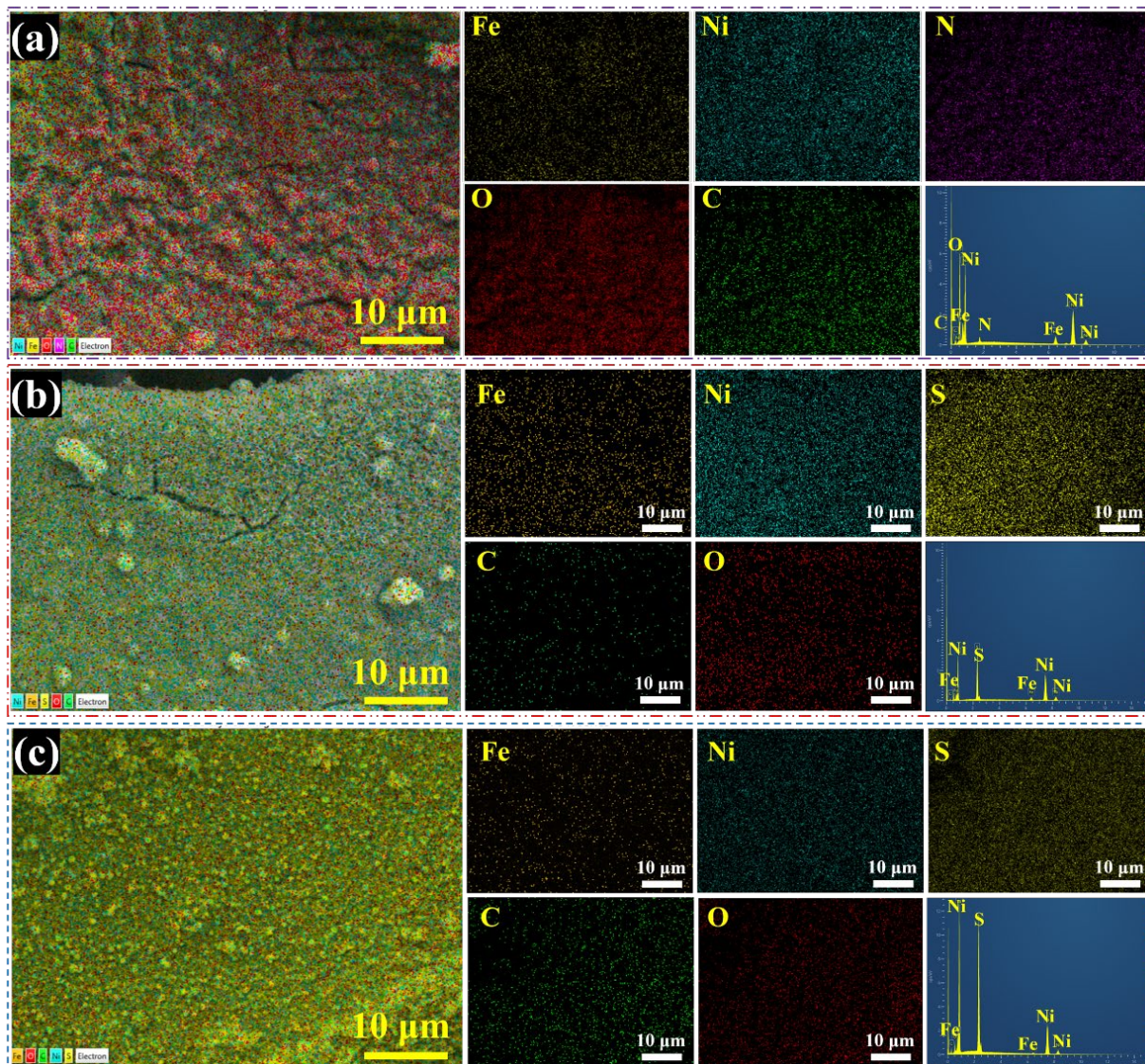


**Figure S2.** EDS elemental color mapping shows the presence of different elements, corresponding EDS spectrum and EDS elemental spectrum plots of (a)FNM, (b) FNMS, and (c) FNMOS samples.



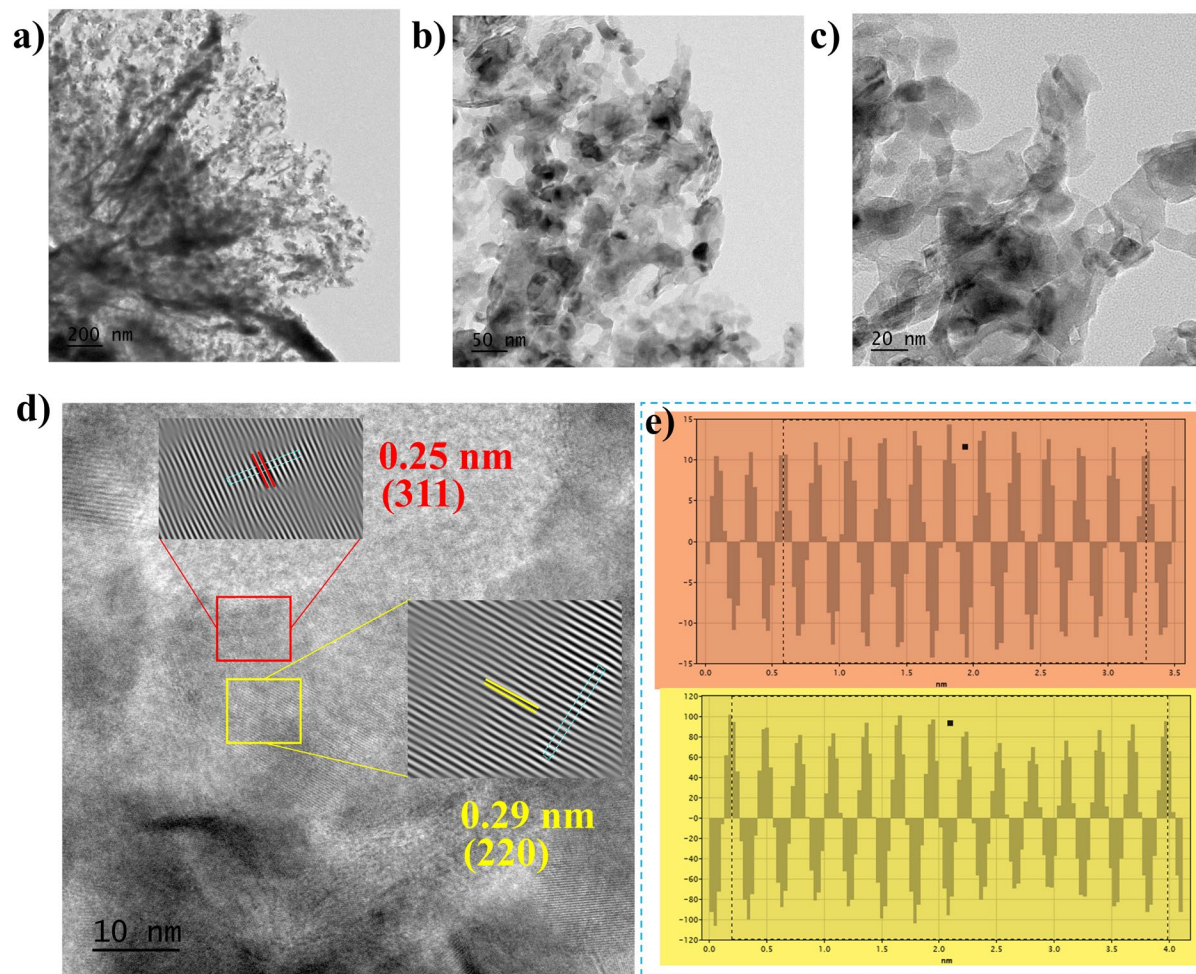


**Figure S3.** (a-d) TEM and HR-TEM images of the FNMO sample (e) line profiles of the selected IFFT spectrums.

**Table S1.** The weight percentage of different elements in FNM, FNMS, and FNMOS electrodes.

<b>At%</b>	<b>FNM</b>	<b>FNMS</b>	<b>FNMOS</b>
<b>Fe</b>	4	3.1	0.6
<b>Ni</b>	36.5	55.6	37.1
<b>O</b>	39.8	6.2	9.0
<b>C</b>	19.0	13.0	26.8
<b>N</b>	0.7		
<b>S</b>		19.3	29.3

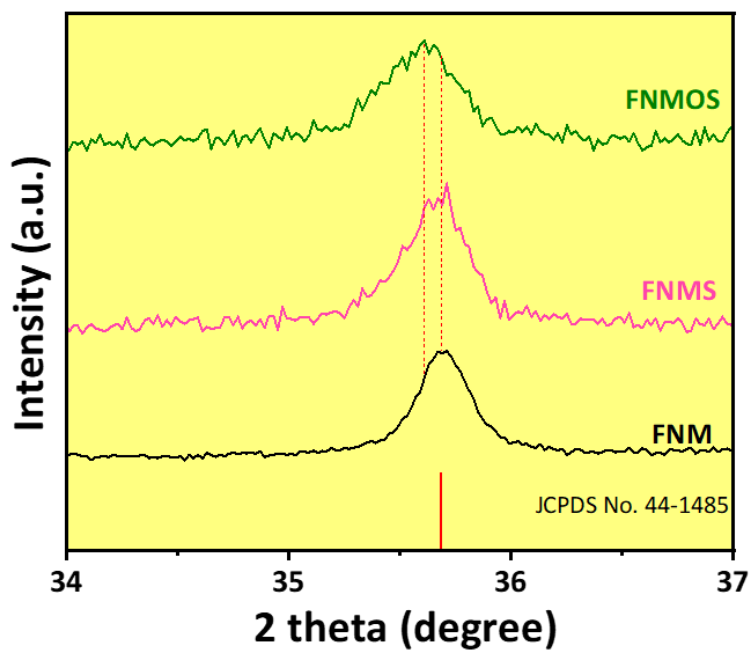


**Figure S4.** XRD pattern of FNMS and FNMOS ranging from 34-38 two theta.

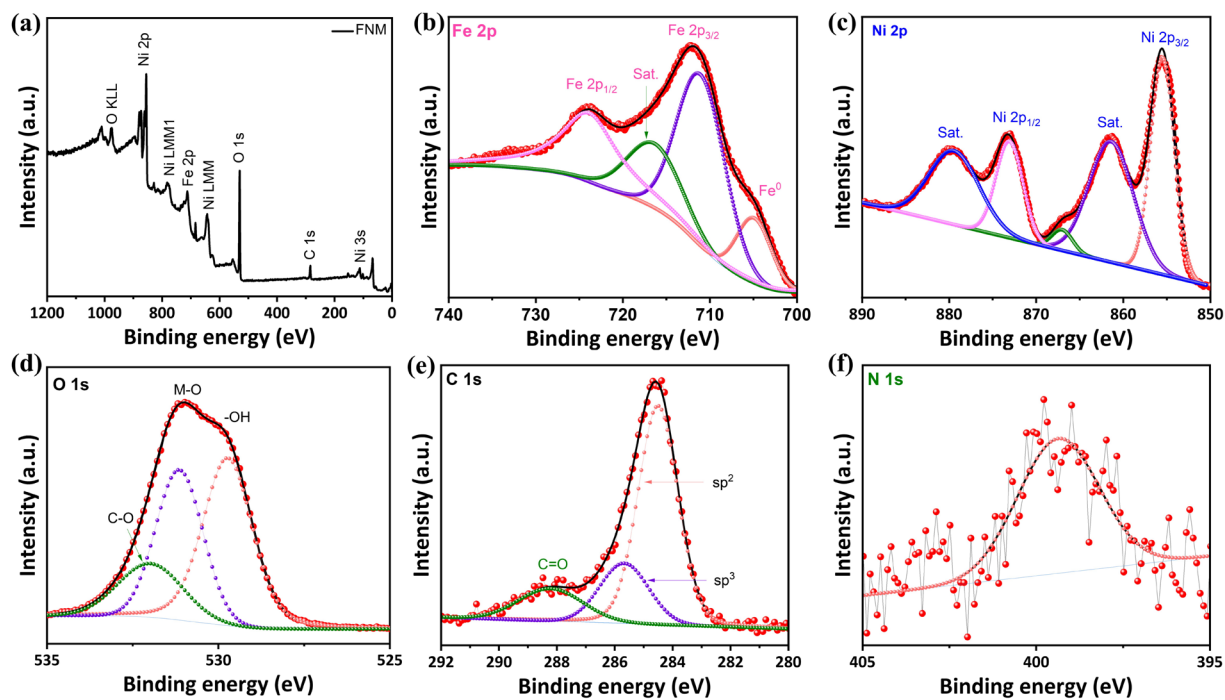


**Figure S5.** XPS profiles of (a) FNM survey, (b) Fe 2p, (c) Ni 2p, (d) O 1s, (e) C 1s, and (f) N 1s.

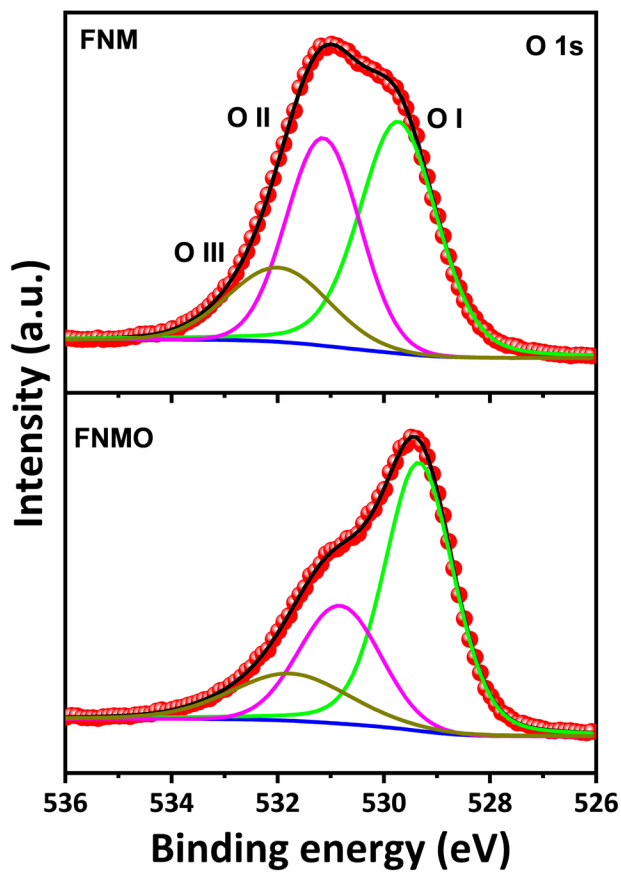


**Figure S6.** Comparative XPS spectra of FNM and FNMO O 1s.

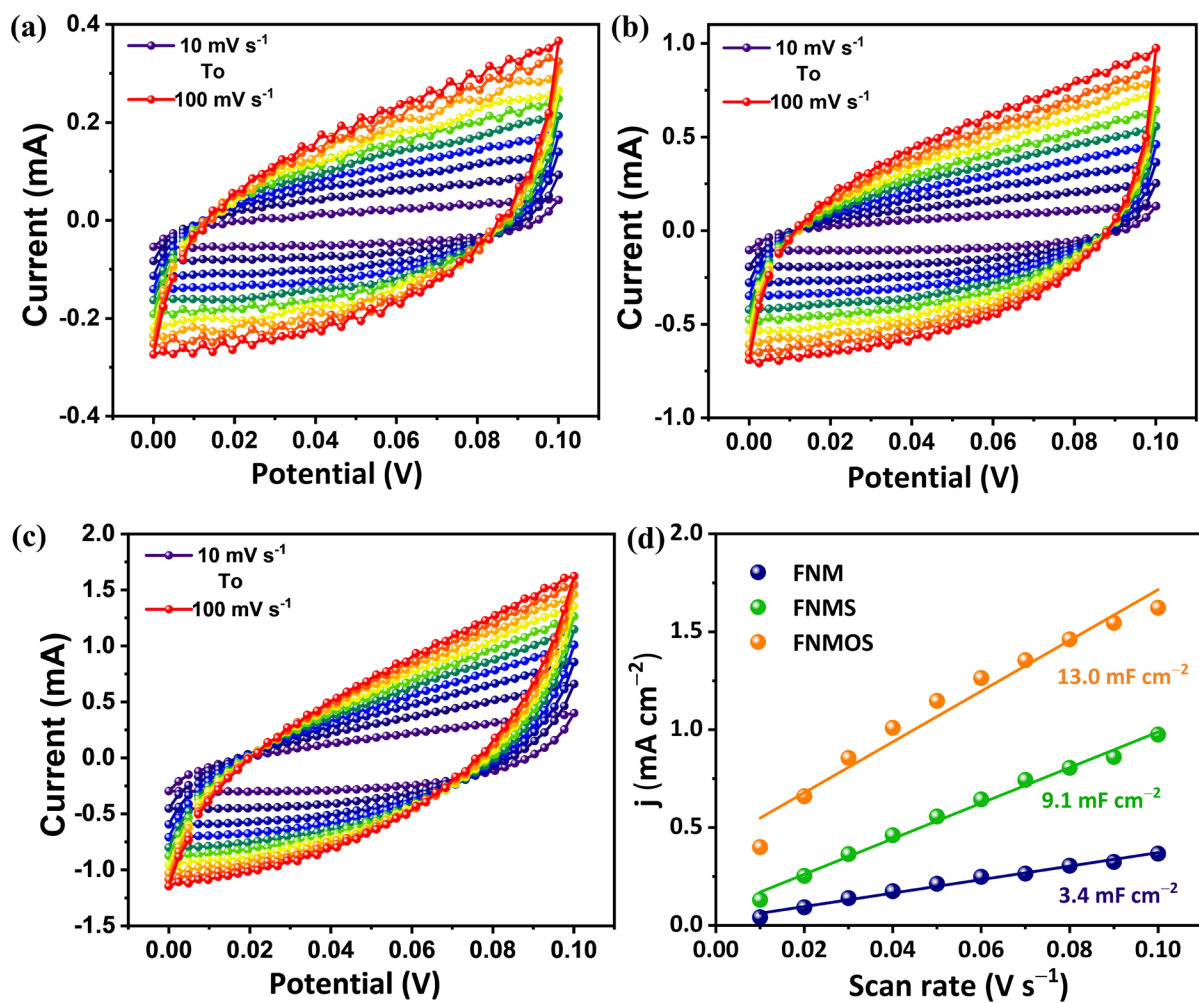


**Figure S7.** CV curves of different electrodes over non-faradaic regions at various scan rates. (a) FNM, (b) FNMS, (c) FNMOS. (d) double-layer capacitance measurements of respective electrodes.

**Table S2.** Diffusion and capacitive contribution percentage of different electrodes.

FNM		FNMS		FNMOS	
Diffusion (%)	Capacitive (%)	Diffusion (%)	Capacitive (%)	Diffusion (%)	Capacitive (%)
38.3	61.7	41.3	58.7	53.2	46.8
27.3	72.7	40.3	59.7	43.6	56.4
22.9	77.1	38.9	61.1	39.7	60.3
20.6	79.4	37.6	62.4	40	60

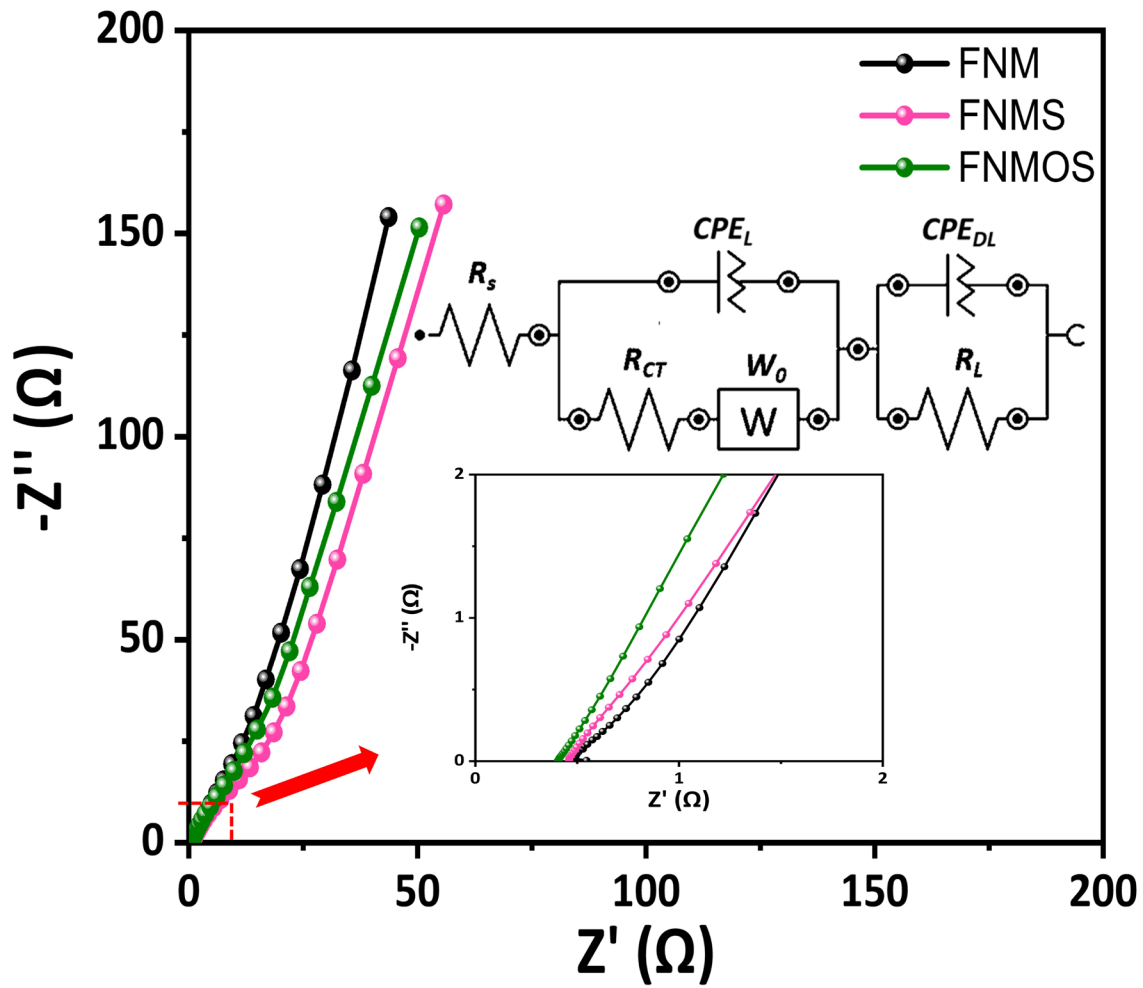
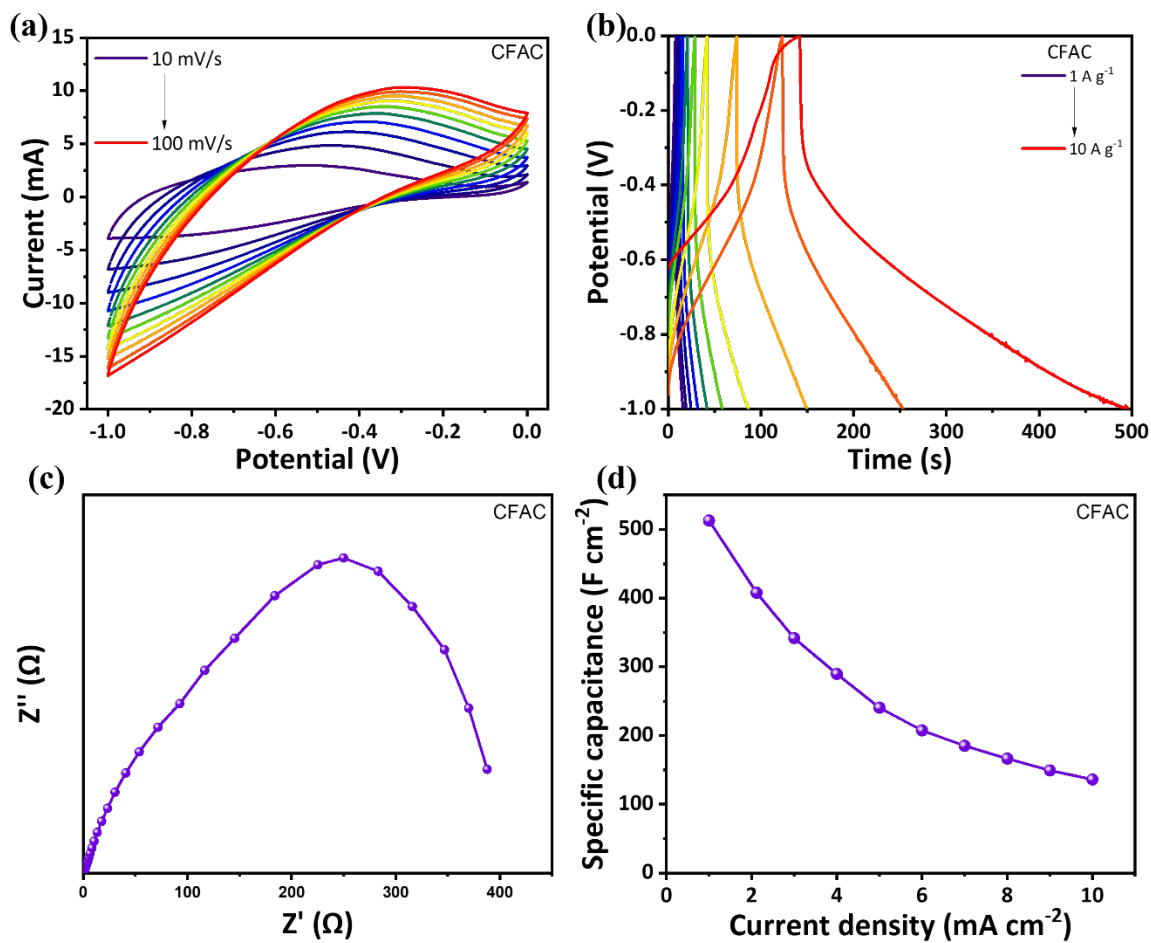
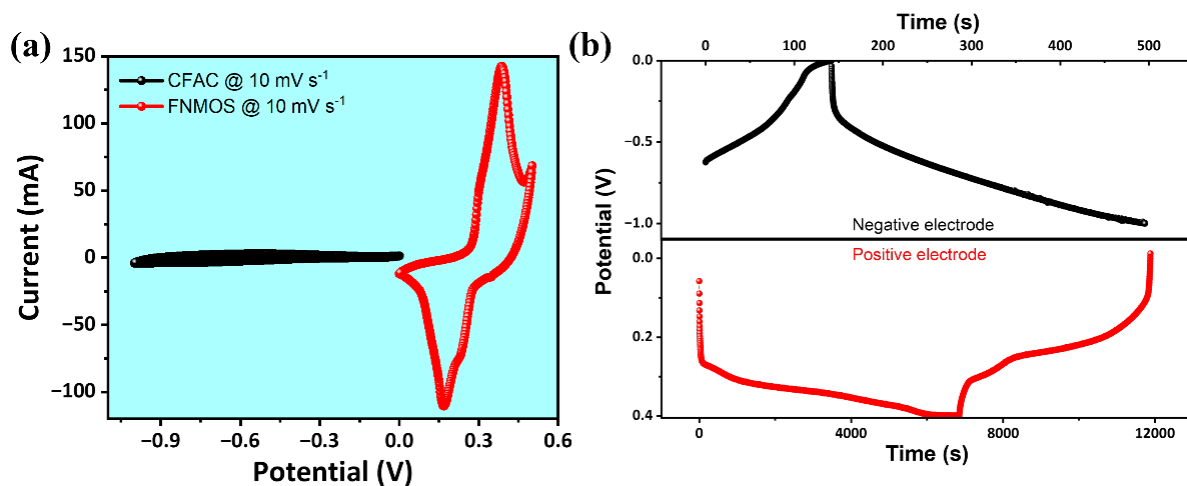


Figure S8. EIS spectrum of different electrodes along with equivalent electrical circuit.





**Figure S9.** (a) CV, (b) GCD, (c) EIS, and (d) specific capacitance plots of CFAC negative electrode.



**Figure S10.** (a) CV curves of CFAC negative electrode and FNMOS positive electrode at 10 mV s<sup>-1</sup> scan rate, (b) Comparison of the discharge plot of the CFAC negative electrode and FNMOS positive electrode at a current density of 1 mA g<sup>-1</sup> and 1 mA cm<sup>-2</sup> respectively.

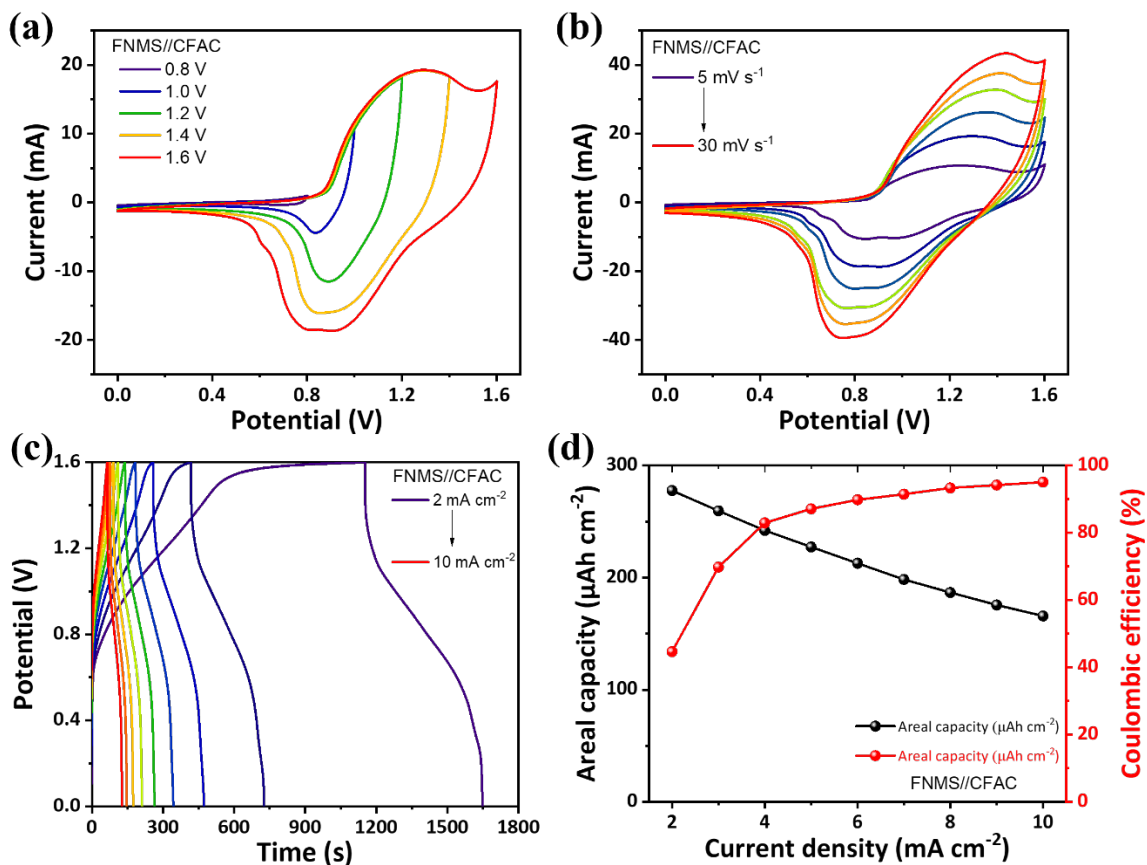


**Figure S11.** ASCD performance of FNMS//CFAC, **(a)** CV curves over different potential windows all conducted at 10 mV s<sup>-1</sup>, **(b)** CV curves at different scan rates within the potential window of 0–1.6 V, **(c)** GCD curves over different current densities, **(d)** area specific capacity and coulombic efficiency over different scan rates.

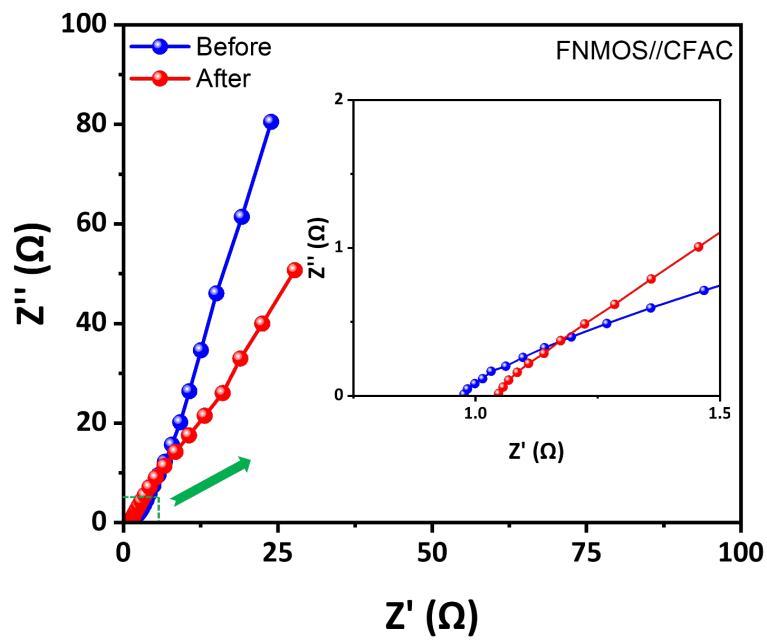


**Figure S12.** EIS spectrum of the FNMOS//CFAC ASCD before and after the 25,000 GCD test.